AUSTRALIAN ATOMIC ENERGY COMMISSION

RESEARCH ESTABLISHMENT

LUCAS HEIGHTS

TRANSIENT CAPACITANCE MEASUREMENTS OF DEEP LEVEL DEFECTS INTRODUCED IN γ-RAY COMPENSATED GERMANIUM BY LONG-TERM ANNEALING AT ROOM TEMPERATURE

by

S.J. PEARTON
A.A. WILLIAMS
A. J. TAVENDALE
E.M. LAWSON

September 1980

AUSTRALIAN ATOMIC ENERGY COMMISSION
RESEARCH ESTABLISHMENT
LUCAS HEIGHTS

TRANSIENT CAPACITANCE MEASUREMENTS OF DEEP LEVEL
DEFECTS INTRODUCED IN Y-RAY COMPENSATED GERMANIUM
BY LONG-TERM ANNEALING AT ROOM TEMPERATURE

by

S.J. PEARTON*
A.A. WILLIAMS
A.J. TAVENDALE
E.M. LAWSON

ABSTRACT

Deep level transient spectroscopy (DLTS) has been applied to defect centres in Y-ray compensated germanium that has been subjected to long-term annealing at room temperature. Deep donor levels (E_c - 0.36 eV, E_c - 0.20 eV) have been observed for the first time; annealing at 675°C for 3 hours increased their concentration in proportion to the free carrier density, indicating stable defect-impurity complexes. Recently irradiated samples from the original material have not shown these levels. The results support Russian work on the compensation mechanism - the formation of electrically inactive vacancy-donor complexes.

* AINSE Postgraduate student on attachment to the AAEC from the Physics Department, University of Tasmania

The following descriptors have been selected from the INIS Thesaurus to describe the subject content of this report for information retrieval purposes. For further details please refer to IAEA-INIS-12 (INIS: Manual for Indexing) and IAEA-INIS-13 (INIS: Thesaurus) published in Vienna by the International Atomic Energy Agency.

EMISSION SPECTROSCOPY; GERMANIUM; SEMICONDUCTOR MATERIALS; VACANCIES; RADIATION EFFECTS; GAMMA RADIATION; ANNEALING

CONTENTS

1. INTRODUCTION

Deep level transient spectroscopy [DLTS: Lang 1974a,b] offers several advantages over more traditional methods of detection of deep level defects in semiconductors; these include high sensitivity (levels down to 10^{-4} of the net background doping density), good resolution, and scanning of the whole bandgap, over a period not exceeding one hour, for both electrons and holes.

Deep level transient spectroscopy has been applied for the first time in the study of radiation induced defect levels in γ-ray compensated Ge. Acceptor defects introduced by irradiation provide compensation of the donors in the original n-type material, allowing thick ($\sim$mm) depletion regions to be established and hence adequate sensitive volumes for nuclear γ-ray detectors. The ability to produce practical nuclear radiation detectors by γ-compensation would obviate the need for the time-consuming and uncertain lithium-ion drift process, and hence the need to store detectors at liquid N_2 temperature. High purity Ge diodes have this advantage, but the crystals are expensive and difficult to grow, and the γ-compensation method, if successful, could 'rescue' moderately pure n-type crystals for radiation detection. The disadvantage of compensation by irradiation is the introduction of primary defect centres deep in the forbidden band which may trap charge released by incident ionising radiation, producing a deleterious effect on the resolution of the detector.

This report gives results of the measurements of defect characteristics in γ-ray compensated germanium that has been subjected to long-term annealing, and demonstrates the power of DLTS as an investigative tool for radiation-induced, deep-level, electrically-active defect centres in semiconductor detectors.

2. PREVIOUS WORK

Radiation damage in semiconductors ¿is complex because of the competing interactions among primary (or radiation-induced) defects, and between these defects and chemical impurities and lattice imperfections. The nature and defect structures of many of the different energy levels introduced into the forbidden band are not known.

Previous methods of deep level detection (e.g. Hall effect measurements, photoluminescence, thermally stimulated current and capacitance) were unable to observe deep level defect centres accurately. Together with the complexity of the defect interactions, and this dependence on experimental conditions (temperature, irradiation energy etc.), this has led to some ambivalence as to the true nature of the compensation mechanism. Published results on radiation and annealing studies on germanium, and on Ge(γ) detector performance [Cleland 1972; Cleland et al. 1975; Llacer 1971, 1972] have provided some explanations. Much of the theoretical (and experimental) work on irradiated germanium for γ-ray detectors has been done in the USSR. The detailed mechanism of primary defect-impurity interaction is still unknown, but a semi-quantitative theory relating to the method of compensation exists [Mashovets et al. 1975a,b; Emtzev et al. 1972; Dostkhodzhaev et al. 1977].

It is thought that vacancy (V) or interstitial (I) interaction with group V impurity donor atoms, D (forming electrically inactive V-D complexes), is the main process leading, in some cases, to compensation (at a certain ratio of group V donor atom concentration to other impurity atom concentrations), and may be neglected under other conditions. For large concentrations of oxygen or silicon impurities, the 'usual' compensation of the shallow donors by the oxygen-related acceptor level at $E_V + 0.27$ eV, or the silicon-related acceptor states at $E_V + 0.34$ eV, takes place. For the conditions under which the removal of group V atoms into neutral complexes is the main compensating process, acceptor levels in the lower half of the gap may be produced after n-p conversion by vacancy-trapping by the V-D complex (divacancy-donor formation).

At least two types of radiation-induced defects are found before n-p conversion: (i) the neutral V-D centres; and (ii) an acceptor state at $E_c - 0.2$ eV which is most probably due to one of the configurations of an interstitial group V atom D_I. The other configuration and that of the self-interstitial Ge_I are thought to provide donor defect levels at or near mid-gap. After n-p conversion, the self-interstitial is in the electrically inactive (in p-type) state. Others [Cleland 1975; Gerasimov et al. 1978] have assigned the $E_c - 0.20$ eV level to a substitutional group V donor-vacancy complex (D_S-V).

Annealing of material which retains n-type conduction after irradiation is explained by the simultaneous disappearance of the V-D complexes and the D_I impurity. Recombination occurs due to the return of the D_I atom to a

substitutional lattice site $(D_I \longrightarrow D_S)$ followed by Ge_I + (V-D) D_S; such a mechanism would produce two donors. A review of the knowledge of point defects introduced into germanium by irradiation has been published by Mashovets [1977]. Table 1 gives energy levels obtained by other workers for defect and impurity centres in germanium.

3. EXPERIMENTAL PROCEDURE

3.1 Sample Preparation

The samples used are of interest because of the time lapse since their irradiation (approximately 10 years). Considerable annealing at room temperature may have occurred during this period. The material parameters, contact preparation and detector characterististics have been described elsewhere [Lawson 1969]. Briefly, the diodes were originally zone levelled n-type Ge with a resistivity of 25-30 Ω cm corresponding to a net donor density of 5 x 10^{13} cm^{-3}. Contacts were formed by lithium diffusion (n$^+$ contact, thickness approximately 300 μm) by evaporation from a metallic lithium source, and Au or Pd evaporation to provide the rectifying contact (approximately 20 nm thickness). The n$^+$ contacts were still stable 10 years after their preparation, indicating the complexing of lithium into stable Li-O pairs. After testing on the DLTS system, the original barriers were polished off with a slurry of 600 grade SiC grit on pile cloth, the samples etched in a 4:1 mixture of HNO_3 (70 wt %) and HF (40 wt %) and new gold or palladium barriers evaporated onto the samples. This was to ensure that barrier damage or surface effects were not responsible for any of the observed peaks (since the samples depleted from the Au contact). The diodes were then re-tested, and the same peaks recorded, though some surface-related peaks had changed in relative magnitude. For samples annealed at 675°C, both contacts were lapped off, and the diodes remade after the annealing period. Irradiations (1969 and 1979) were performed in a 21 kGy h^{-1} (2.1 Mrad h^{-1}) facility.

To perform the DLTS scans, the samples were mounted in an Oxford Instruments CF-100 continuous flow cryostat. The sample holder was surrounded by a cooled, polished copper radiation shield for liquid helium work. The temperature was measured with a gold (0.03 atomic per cent iron)/chromel thermocouple which has a high sensitivity at LHe temperatures (15 μV K^{-1}). The reference junction was maintained at the boiling point of liquid N_2. Samples were mounted on a sapphire plate in which the thermocouple was

embedded.

3.2 DLTS Measurements

A depletion layer devoid of free carriers was established in the sample by application of a fixed reverse bias. By repetitively pulsing the sample diode toward or into forward bias, a trap spectrum was obtained on scanning from reference temperature (4.2 K or 77 K) to room temperature. A peak in the spectrum was produced when the carrier emission rate from the particular trap in the depletion layer matched an internally generated decaying exponential waveform (weighting function) produced by an electronic correlator [Miller et al. 1975]. A Boonton bridge (Model 71A) operating at 1 MHz measured the test device capacitance. Minority carrier injection is impossible with Schottky barrier structures, so a light emitting diode (LED) was used to introduce minority carriers when measuring hole traps. An X-Y recorder with the facility of variable signal integration plotted the correlator output against temperature. A block diagram of the system is shown in Figure 1.

Since the thermal emission rate $e_n(e_p)$ of an electron (hole) trap depends exponentially on absolute temperature T (see review by Miller et al. [1977])

$$e_n = \frac{\sigma_n \langle v_n \rangle N_c}{g} \exp\left(-\frac{\Delta E}{kT}\right) \tag{1}$$

where σ_n = capture cross section of trap for electrons, $\langle v_n \rangle$ = average thermal velocity of free carrier, N_c = density of states in conduction band, g = degeneracy of level (unknown for deep traps and assumed to be 2), ΔE = energy difference of trap from conduction band, k = Boltzmann's constant, T = absolute temperature, and the energy separation of the defect level from the appropriate band edge may be obtained by measuring the thermal emission rate as a function of temperature. A correction must be applied to the calculated value to account for the T^2 dependence of the exponential prefactor. As discussed by Miller et al. [1977], the simplest method is to subtract $2kT$, where T is the average temperature of the peak over the range of time constants. The condition for obtaining the activation energy for electron emission from a trap, $e_n \gg e_p$, was checked by observing the constancy of the transient capacitance change over the range of time constants (5-100 ms). (The time constant actually measured is $(e_n + e_p)^{-1}$, but for electron traps usually $e_n \gg e_p$, and conversely for hole traps.)

Capture cross sections may be measured by following the capacitance signal output after the pulse as a function of the pulse duration. The capture of the free carriers occurs in the neutral material because of the decrease in space-charge (depletion) width during the bias pulse. The peak height of the DLTS signal is related to the pulse width t by

$$n(t) = N_T (1 - \exp(^{-t}/\tau)) \tag{2}$$

where τ^{-1} = rate of carrier capture by trap, and N_T = trap concentration. The cross section is obtained from the expression

$$\tau^{-1} = \langle v \rangle n \sigma \tag{3}$$

where n = net background doping density. The method is straightforward for majority carrier traps, but poses problems for minority carriers because the injection efficiency of a forward biasing (or LED) pulse is generally unknown, hence the injected carrier density is subject to large calculational errors. In the present case, minority carrier cross sections have been derived from the exponential prefactor of the thermal emission rate. This method is subject to large uncertainties because the factors involved may include field and temperature dependences, but, in the cross sections directly measured, no temperature dependences were observed, and results were checked at several biases and indicated no voltage dependence. This may be expected because the peaks shift by only approximately 15 K over the set of time constants, and the electric fields are low (20 V cm^{-1} - 120 V cm^{-1}). The discrepancy between directly measured and derived cross sections is not yet understood but it may be related to the fact that pulsed bias methods measure cross sections for neutral material, whereas derived values are obtained from thermal emission rates measured in the space-charge region.

Trap concentrations are obtained by measuring the relative change in capacitance signal produced by a small change in the pulse amplitude, V. The defect concentration, N_T, may be profiled using [Lang 1974a,b]:

$$\delta \left(\frac{\Delta c}{c} \right) = \left(\frac{\epsilon}{qw^2 n} \right) \frac{N_T(x)}{n(x)} \delta V \tag{4}$$

where q = electronic charge, w = depletion layer width, ϵ = dielectric constant, n(x) = free carrier density at depth x, and n = free carrier density at edge of depletion region. If a plot of Δc against pulse amplitude is linear, the trap concentration profile is the same as that of the free carrier

density profile. An approximation, valid for Δc/c << 1 and the one-sided abrupt junction assumption, is

$$N_T \approx 2n\,\frac{\Delta c}{c} \tag{5}$$

where c = capacitance of the device at the quiescent reverse bias, and Δc = change in capacitance produced by pulsing to zero bias.

Electric field enhancement of emission rates may be checked by repeating measurements at various standing biases, and spatial variations in emission rate due to inhomogeneous material determined by following the profiling procedure.

4. RESULTS

Measurements of thermal emission rate as a function of temperature were made on three diodes which had been subjected to long-term annealing at room temperature. One of these (4D2) was then annealed for three hours at approximately 900°C and re-tested. Following this, the diode, along with three previously unirradiated samples from the original material, was irradiated to a dose of 1500 kGy (150 Mrad). One of the latter samples (5A) was annealed at 675°C under H_2 for three hours after testing to determine whether deep donors could be introduced by the thermal anneal. Trap energies, concentrations and cross sections were obtained as outlined above (Section 3). The data are summarised in Table 2. Energies obtained by estimation from the peak position assumed a temperature independent value of $\sigma = 10^{-14}$ cm^2 in Equation (1) - directly measured cross sections of other traps showed no temperature dependence. This procedure was used in cases where data were difficult to obtain because of peak interference or low signal-to-noise ratio. Typical values for the most probable errors arising from curve fitting are 7 per cent for energies, 30 per cent for cross sections and 25 per cent for concentrations. Defects are labelled by their peak temperature position for a correlator time constant of 10 ms. The peak position is averaged over an up-and-down temperature scan.

Figures 2-6 show DLT spectra from the three diodes evidencing the E_c - 0.36 eV donor level. Two of these diodes were compensated (net donor density sample 4D2 $\approx$ 5.9 x 10^{10} cm^{-3}, sample 2B $\approx$ 2.4 x 10^{10} cm^{-3}) and the other partially compensated (net donor density sample 5D $\approx$ 9.9 x 10^{12} cm^{-3}). Figure

7 shows typical data used to obtain capture cross sections and Figure 8 the Arrhenius plot of the data for the E_c - 0.36 eV level. Figure 9 shows that the concentration of this defect has a flat profile, i.e. it is constant over the region of the diode investigated, and Figure 10 is a typical plot of data used to obtain the net free carrier density of the samples under test. The devices were checked for conductance type by observing their response at low bias to impinging α-particles. All retained n-type conductance.

5. DISCUSSION

Table 1 shows a compilation of published results on γ - and electron-irradiated germanium, and levels introduced by various common impurities. The impurity correlations can be regarded as only tentative in most cases. Results have been obtained by a variety of methods including Hall effect measurements, DLTS and photoluminescence. Russian models [Emtzev et al. 1971, 1972; Goncharov et al. 1977; Mashovets et al. 1975a,b] of the defect mechanism have envisaged interstitial group V donor impurities causing two levels, one an acceptor state at E_c - 200 meV and the other a donor level near midgap. The germanium interstitial is also thought to cause a donor level at midgap.

Table 2 shows that the E_c - 0.36 eV level appeared in all of the samples which had undergone long-term annealing at room temperature. It did not appear in the unirradiated original material, nor in the offcuts which were subsequently irradiated. The level could not be removed by annealing at approximately 900°C and, in fact, its concentration increased in ratio to the free carrier density. Conversely, the deep donor could not be introduced by thermal annealing at 675°C. It appears that the level can only be introduced in irradiated material which has undergone considerable annealing at room temperature, and that this process leads to the formation of extremely stable impurity-defect complexes. Spark source mass spectrometry of zone refined germanium bars has revealed silicon concentrations of approximately 10^{16} cm^{-3}, and photothermal ionisation spectroscopy studies have revealed phosphorus as a common impurity in germanium (AAEC work, unpublished).

The stability of the deep donor levels formed, and their concentrations, may indicate either a stable oxide involving silica and/or phosphorus, or possibly a complex involving impurities such as silicon and phosphorus and a radiation defect, e.g. Si-P (V). Some of the shallower donor levels and the

absence of the E_c - 0.2 eV acceptor level could be explained then in terms of the model of Mashovets and colleagues by assuming several different group V impurities present in the original material. The incorporation into the lattice of a group V interstitial and a vacancy-donor complex would cause the appearance of two spatially separated donors. Thus the diodes would retain n-type conductance. The other donor levels observed are not identified but clearly, from the results on the unirradiated material, they result from complexing of radiation-induced defects with chemical impurities originally present. Despite the fact that oxygen was thought to be present because of the stability of the Li n^+ contacts, no definite oxygen-related peaks were observed. The newly irradiated material will be checked at regular intervals for evidence of the formation of the E_c - 0.36 eV level.

6. SUMMARY

Deep donor levels in γ-irradiated n-type Ge have been observed for the first time using DLTS. Annealing at room temperature introduces a deep donor level at E_c - 0.36 eV in all samples and at E_c - 0.20 eV in some samples. These were not observed in recently irradiated samples from the same material. Trap densities several orders of magnitude lower than the original doping density of the material were found, supporting the hypothesis of electrically inactive vacancy-donor complexing.

The implication of these results for Ge(γ) detectors is that they may have a short useful lifetime at room temperature (possibly of the order of months) before the radiation-induced compensating acceptors are annealed, leading to the formation of extremely stable donor complexes. If this is the case, detectors fabricated by this technique may have to be stored at liquid nitrogen temperatures, removing their single biggest advantage, the possibility of room temperature storage of a low cost germanium detector.

7. ACKNOWLEDGEMENTS

8. <u>REFERENCES</u>

[1] Akimchenko, I.P., Vavilov, V.S. and Plotnikov, A.F. [1963] - Fiz.
     Tverd. Tela, (5) 1417 (Sov. Phys. - Solid State, 5:1031-5 (1963)).

[2] Arli, N.B., Desnica, U.V., Riepe, G. and Protic, D. [1972] - Radiation
     damage and defects in semiconductors. Institute of Physics Conf. Series
     No.16, p.341.

[3] Basman, A.R., Gerasimov, A.B., Kakhidze, N.G., Konovalenko, B.M. and
     Tsertsvadge, A.A. [1974a] - Sov. Phys. - Semicond., 7(7)903.

[4] Basman, A.R., Gerasimov, A.B., Gogotishvili, M.K., Dolidge, N.D.,
     Kasparyan, K.I., Kakhidze, N.G. and Konovalenko, B.M. [1974b] - Sov.
     Phys. - Semicond., 7(7)922.

[5] Borodovskii, Y.A., Gavrilov, G.M., Goncharov, L.A., Kervalistivili,
     P.D., Litovchenko, P.G., Khorvat, A.M. [1977] - Sov. Phys. - Semicond.,
     11(10)1180.

[6] Cleland, J.W., Crawford, J.H.J. and Holmes, D.K. [1956] - Phys. Rev.,
     102:722.

[7] Cleland, J.W. [1972] - IEEE Trans. Nucl. Sci., 19:224.

[8] Cleland, J.W., James, F.J. and Westbrook, R.D. [1975] - IEEE Trans.
     Nucl. Sci., 22(6)2289.

[9] Curtis, O.L. and Crawford, J.H. Jr. [1961] - Phys. Rev., 124:1731.

[10] Dostkhodzhaev, T.N., Emtzev, V.V., Korchazhkina, R.L. and Mashovets,
     T.V. [1977] - Sov. Phys. - Semicond., 11(11)1249.

[11] Emtzev, V.V., Mashovets, T.V., Maximov, M. and Vitovskii, N.A. [1971]
     - Radiation Effects in Semiconductors (eds. J.W. Corbett and G.D.
     Watkins), Gordon and Breach, London.

[12] Emtzev, V.V., Mashovets, T.V. and Ryvkin, S.M. [1972] - Radiation
     damage and defects in semiconductors. Institute of Physics Conf.
     Series No.16, p.17.

[13] Gremin, V.K., Danengirsh, S.G., Strokan, N.B., Tisnek, N.I. and Turebekov, U.Sh. [1977] - Sov. Phys. - Semicond., 11(6)704.

[14] Evwaraye, A.O., Hall, R.N. and Soltys, T.J. [1979] - IEEE Trans. Nucl. Sci., 26(1)271.

[15] Fukuoka, N., Saito, H. and Tutsumi, Y. [1972] - Radiation damage and defects in semiconductors. Institute of Physics Conf., Series No.16, p.328.

[16] Gerasimov, A.B., Gogotishvili, M.K., Dolidge, N.D., Konovalenko, B.M. and Mayradze, M.V. [1978] - Sov. Phys. - Semicond., 12(8)878.

[17] Goncharov, L.A., Dostkhodzhaev, T.N., Emtzev, V.V., Mashovets, T.V. and Ryvkin, S.M. [1977] - Sov. Phys. - Semicond., 11(5)556.

[18] Haller, E.E., Hubbard, G.S. and Hansen, W.L. [1977] - IEEE Trans. Nucl. Sci., 24(1)48.

[19] Haller, E.E., Li, P.P., Hubbard, G.S. and Hansen, W.L. [1979] - IEEE Trans. Nucl. Sci., 26(1)265.

[20] Haller, E.E. [1979] - LBL-9901.

[21] Lang, D.V. [1974a] - J. Appl. Phys., 45:3014.

[22] Lang, D.V. [1974b] - J. Appl. Phys., 45:3023.

[23] Laurence, G. and Albany, H.J. [1971] - Radiation Effects in Semiconductors. (eds. J.W. Corbett and G.D. Watkins), Gordon and Breach, London.

[24] Lawson, E.M. [1969] - AAEC/TM527.

[25] Llacer, J. [1971] - BNL 15 643.

[26] Llacer, J. [1972] - IEEE Trans. Nucl. Sci., 19:295.

[27] Mashovets, T.V., Ubdurakhmanova, S.N., Dostkhodzhaev, T.N. and Emtzev, V.V. [1975a] - Sov. Phys. - Semicond., 8(9)1144.

[28] Mashovets, T.V., Ubdurakhmanova, S.N., Vasileva, E.D. and Emtzev, V.V.
      [1975b] - Sov. Phys. - Semicond., 8(9)1139.

[29] Mashovets, T.V. [1977] - Radiation effects in semiconductors.
      Institute of Physics Conf., Series No.31, p.30.

[30] Miller, G.L., Ramirez, J.V. and Robinson, D.A.H. [1975] - J. Appl.
      Phys., 46(6)2638.

[31] Miller, G.L., Lang, D.V. and Kimmerling, L.C. [1977] - Ann. Rev.
      Mater. Sci., pp.377-448.

[32] Srour, J.R. and Curtis, O.L. Jr. [1971] - Radiation Effects in
      Semiconductors. (eds. J.W. Corbett and G.D. Watkins), Gordon and
      Breach, London, p.113.

[33] Vavilov, V.S., Spitsyn, A.V. and Tchickitchev, M.V. [1971] - Radiation
      Effects in Semiconductors. (eds. J.W. Corbett and G.D. Watkins),
      Gordon and Breach, London, p.75.

[34] Whan, R.E. [1965] - Phys. Rev., 140(2A)A690.

[35] Woodbury, H.H. and Tyler, W.W. [1957] - Phys. Rev., 105:84.

TABLE 1

DEFECT LEVELS IN GERMANIUM

Level (meV) A=acceptor D=donor	Impurity Correlation	Reference
10 (D)	e-irradiated	23
17 (A)	CuH_2	18
17.5 (A)	Cu-H	18
20.5 (A)	$CuLi_2$ or CuLiH	18
25 (A)	CuLi, dislocations	18,14
32 (A)	Cu	25,14
37 (A)	High concentration of 'smooth etch pits'	14
40 (A)	Cu	25,18,14
44 (A)	Cu	25,18,14
60.4 (A)	Cu, H	14,19
67.4 (A)	divacancy-H	14,19
68.7 (A)	oxygen	19
80 (A)	V-O	4
83 (A)	High concentration of 'smooth etch pits' vacancy complex	14,13
90 (A)	Vacancy complex	12
90 (D)	Oxygen defect complex, unknown	34,31
100 (A)	P, As, divacancy, V-V-Li	29,3,18
110 (A)	e-irradiated	23
110 (D)	Te	15
120 (A)	Sb	29
140 (A)	-	14
140 (D)	-	33
150 (A)	Ba	17
151.8 (A)	Copper, Li, H.	19
160 (A)	Bi, $(V-O_2)V$, (As_sV-V), e-irradiated	29,3,20
170 (A)	-	2
179.5 (A)	Cu-H	18
180 (A)	Vacancy complex	13
180 (D)	e-irradiated	20
190 (A)	Vacancy complex, Ba-related	13,5
200 (D)	e-irradiated	20
200 (A)	e-irradiated	23
E_c-200 (A)	V-I, group V donors, Sb	29,25
210 (A)	Cu-related	5
220 (A)	(As_sV)	3
230 (D)	-	9
240 (D)	-	33
250 (D)	e-irradiated	20
250 (A)	-,e-irradiated	25,20
260 (A)	Cu	25
E_c-260 (A)	Cu	18

TABLE 1 (Continued)

Level (meV) A=acceptor D=donor	Impurity Correlation	Reference
270 (A)	Vacancy complex, O	3,27
275 (A)	CuLi	18
280 (D)	e-irradiated	20
300 (A)	Cu, Sb	14,19,25
300 (D)	Te, e-irradiated	15,20
330 (A)	Cu, recombination centre in As, Sb doped material	18,32,23
340 (A)	Si	29
340 (D)	e-irradiated	20
350 (A)	e, n-irradiated	9
360 (A)	Vacancy complex, As, Sb doping, Ge$_i$	3,32,1
400 (D)	e-irradiated	20

TABLE 2

MEASURED TRAP PARAMETERS

Sample	Defect	Level (meV)	Cross Section (cm2) Direct Measurement	From Intercept	Concentration (cm^{-3})
Ge 4D2	31	$E_c - 64$	2.4×10^{-4}	1.3×10^{-15}	2.1×10^9
Hoboken 1968	58	$E_c - 100$	2.3×10^{-14}	2.7×10^{-16}	2.2×10^9
n-type	93 (surface)	$E_c - 177$	7.7×10^{-15}	1.0×10^{-16}	5.1×10^9
Czochralski dose					
4400 kGy (440 Mrad)	111	$E_c - 200$	2.9×10^{-14}	8.3×10^{-15}	9.2×10^9
at T=80°C (1969)	148	$E_c - 363$	2.9×10^{-14}	3.5×10^{-14}	1.4×10^{10}
n=5.9 x 10^{10} cm^{-3} (77 K)	110	$E_v +226$	–	1.3×10^{-14}	6.7×10^9
	149	$E_v + 345$	–	8.4×10^{-16}	1.8×10^{10}
	170	$E_v + 371$	–	6.7×10^{-13}	2.5×10^{10}
As above after	96	$E_v + 140$	–	6.4×10^{-15}	1.9×10^{12}
annealing at 900°C	105	$E_c - 200$	1.6×10^{-14}	4.9×10^{-15}	1.4×10^{12}
for 3 hours (1979)	148	$E_c - 360$	1.8×10^{-14}	–	2.2×10^{12}
n=7.2 x 10^{12} cm^{-3} (77 K)					
As above post	Donors				
Irradiation dose	below 77 K				
1500 kGy (150 Mrad)	still present				
at T=25°C (1979)	105	$E_c - 200$	5.9×10^{-15}	–	7.5×10^{11}
n=3.4 x 10^{12} cm^{-3} (77 K)	145	$E_c - 360$	3.9×10^{-14}	4.6×10^{-14}	8.4×10^{11}
	174 (surface)	$E_c - 370$	7.4×10^{-16}	1.4×10^{-17}	9.4×10^{11}

TABLE 2 (Continued)

Sample	Defect	Level (meV)	Cross Section (cm^2)		Concentration (cm^{-3})
			Direct Measurement	From Intercept	
GeIV n	97	$E_v + 140$	–	–	1.8×10^{11}
offcut of above	110	$E_c - 200$	–	5.6×10^{-14}	3.6×10^{11}
original parent material	142	$E_v + 320$	–	3.8×10^{-13}	1.1×10^{12}
pre-irradiation					
n=5.1 $\times 10^{12}$ cm^{-3} (77 K)					
GeIV n post	80	$E_v + 130$ (est.)	–	–	2×10^{10}
irradiation dose					
1500 kGy (150 Mrad)					
at T=25°C (1979)	97	$E_v - 160$ (est.)	–	–	2×10^{10}
n=3.2 $\times 10^{10}$ cm^{-3} (77 K)	179	$E_v + 360$ (est.)	–	–	3×10^{10}
Ge N(?) 29					
Hoboken 1968 n-type	151	$E_c - 350$	2.4×10^{-13}	8.1×10^{-14}	5.0×10^{9}
dose 2840 kGy (284 Mrad)					
at T=25°C (1969)					
n=2.4 $\times 10^{10}$ cm^{-3} (77 K)					
Ge 2E	111	$E_c - 190$	2.7×10^{-14}	1.3×10^{-15}	1.3×10^{11}
offcut of above					
crystal	135	$E_c - 280$	2.6×10^{-13}	6.2×10^{-13}	3.6×10^{11}
pre-irradiation					
n=3 $\times 10^{13}$ cm^{-3} (77 K)	167	$E_c - 330$	1.7×10^{-14}	2.4×10^{-15}	3.9×10^{11}

TABLE 2 (Continued)

Sample	Defect	Level (meV)	Cross Section (cm²) Direct Measurement	Cross Section (cm²) From Intercept	Concentration (cm⁻³)
Ge 2E post	89 (est.)	$E_v + 150$	—	—	2.4×10^{11}
Irradiation dose	99 (est.)	$E_v + 160$	—	—	2.4×10^{11}
1500 kGy (150 Mrad)	124	$E_c - 230$	—	5.6×10^{-17}	2.3×10^{9}
at T=25°C (1979)	127 (est.)	$E_v + 220$	—	—	2.4×10^{11}
n=1.4 × 10¹¹ cm⁻³ (77 K)	140	$E_c - 280$	—	4.3×10^{-15}	4.6×10^{9}
	180	$E_v + 360$	—	—	9.9×10^{11}
Ge N(γ) 5D	35	$E_c \sim 61$	1.9×10^{-14}	5.9×10^{-15}	4.1×10^{10}
Hoboken 1968	46	$E_c - 75$	1.4×10^{-14}	1.3×10^{-14}	3.6×10^{11}
n-type	63	$E_c - 112$	1.0×10^{-14}	6.7×10^{-15}	2.6×10^{11}
Dose 4100 kGy (410 Mrad)	92 (surface)	$E_c - 215$	8.9×10^{-15}	1.0×10^{-14}	2.7×10^{11}
at T=80°C (1969)	114	$E_c - 196$	7.0×10^{-15}	1.2×10^{-14}	1.6×10^{11}
n=9.9 × 10¹² cm⁻³ (77 K)	155	$E_c - 358$	9.4×10^{-15}	2.3×10^{-14}	1.4×10^{12}
	96	$E_v + 221$	—	8.4×10^{-13}	8.2×10^{11}
	141	$E_v - 321$	—	4.0×10^{-14}	9.9×10^{11}
Ge 5A	134	$E_c - 280$	7.7×10^{-15}	3.2×10^{-15}	4.5×10^{10}
Offcut of above	139	$E_v + 340$	—	3.8×10^{-13}	2.7×10^{11}
crystal	179 (surface)	$E_c - 330$	4.2×10^{-15}	2.4×10^{-15}	3.0×10^{10}
pre-irradiation					
n=1.0 × 10¹³ cm⁻³ (77 K)					

TABLE 2 (Continued)

Sample	Defect	Level (meV)	Cross Section (cm^2)		Concentration (cm^{-3})
			Direct Measurement	From Intercept	
Ge 5A post	126 (est.)	E_v + 220	–	–	7.0×10^{10}
Irradiation	156 (est.)	E_v + 350	–	–	7.2×10^{10}
Dose 1500 kGy (150 Mrad)	180 (est.)	E_v + 370	–	–	6.6×10^{11}
at T=25°C (1979)					
n=8.2 $\times$ 10^{10} cm^{-3} (77 K)					
=1.2 $\times$ 10^{11} cm^{-3} (156 K)					
=1.0 $\times$ 10^{12} cm^{-3} (180 K)					
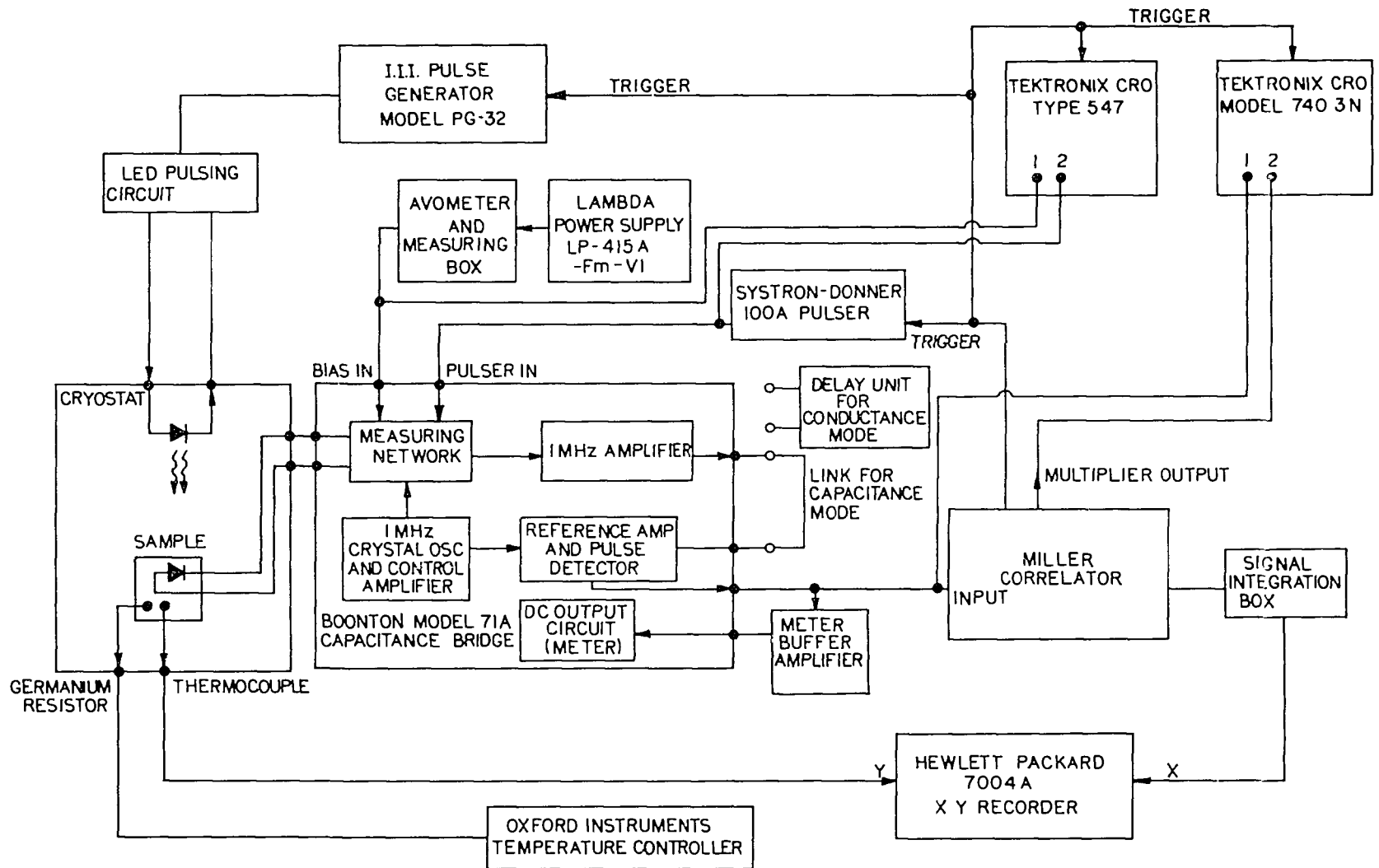
FIGURE 1. BLOCK DIAGRAM OF THE DLTS SYSTEM

19
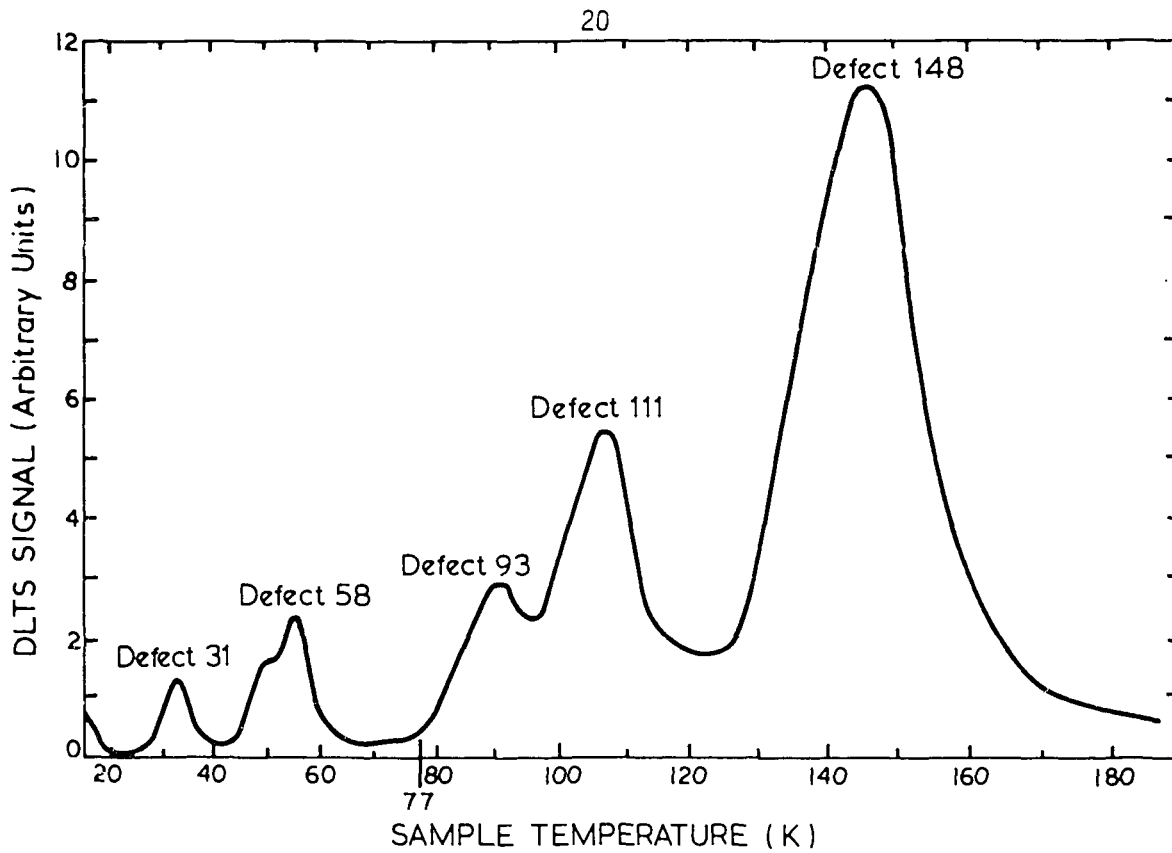
FIGURE 2. DLT SPECTRA OF SAMPLE Ge 4D2 AFTER IRRADIATION
AND THEN 10 YEARS AT ROOM TEMPERATURE.
CORRELATOR TIME CONSTANT τ_c = 10 ms
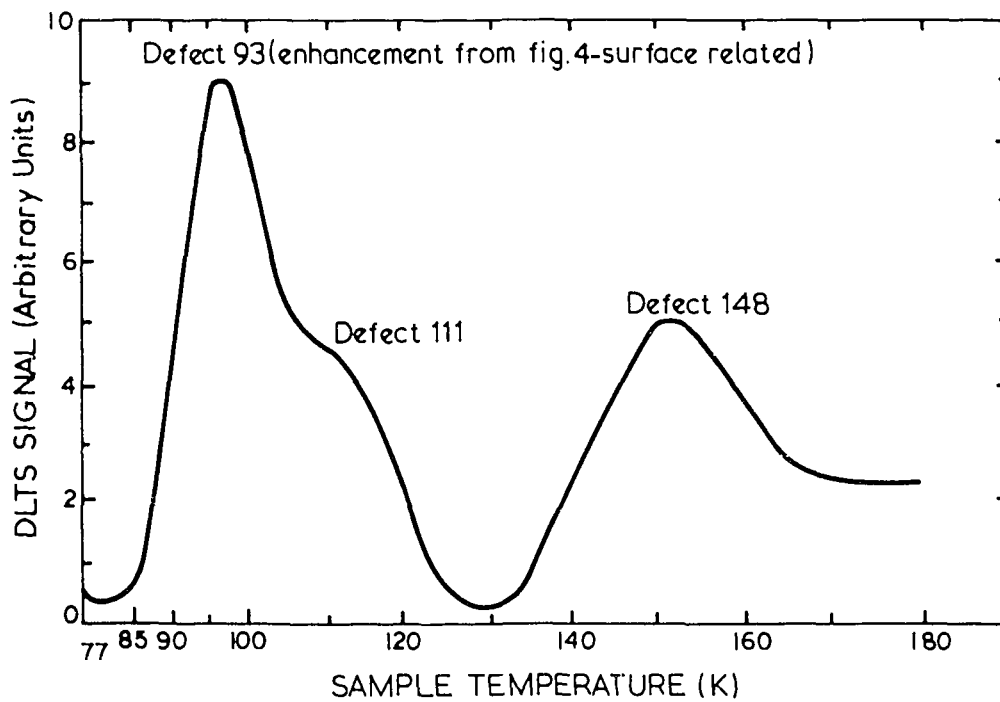
FIGURE 3. DLT SPECTRA OF SAMPLE Ge 4D2 AFTER RE-ETCHING
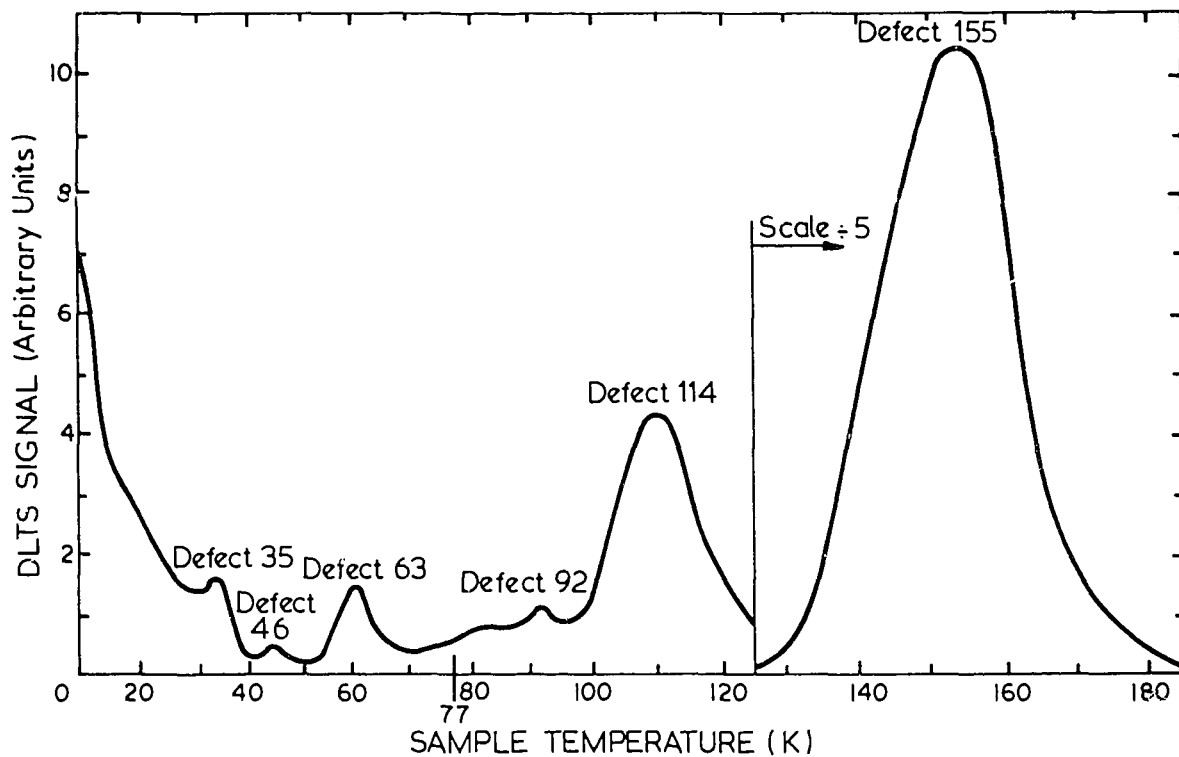AND EVAPORATION OF NEW Au BARRIER. (τ_c = 10 ms)

FIGURE 4. DLT SPECTRA OF SAMPLE Ge 5D AFTER IRRADIATION AND
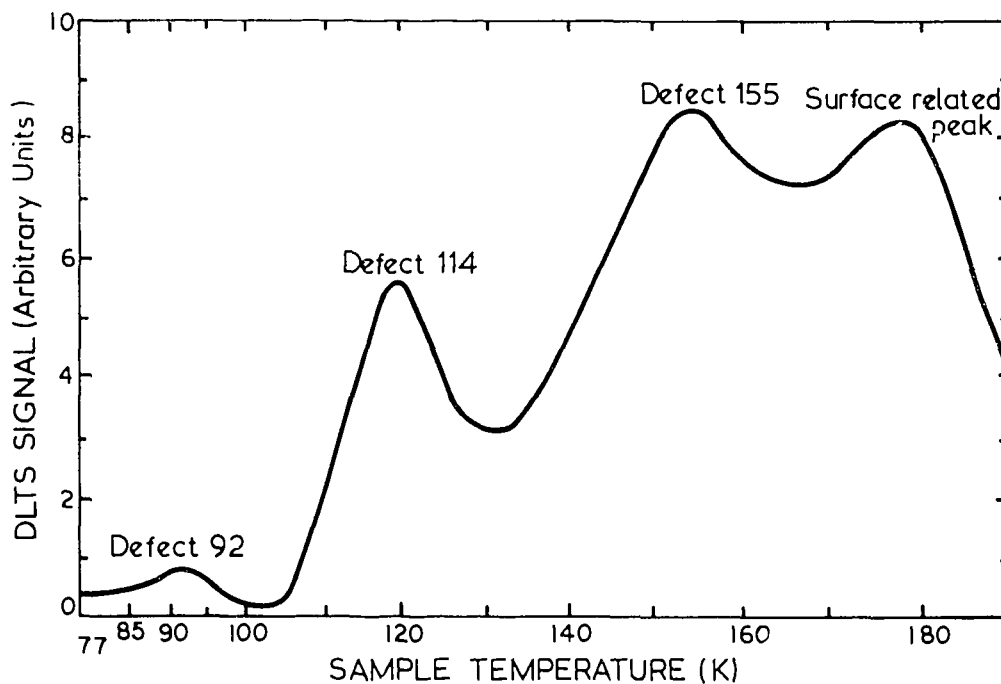THEN 10 YEARS AT ROOM TEMPERATURE. (τ_c = 10 ms)

FIGURE 5. DLT SPECTRA OF SAMPLE Ge 5D AFTER RE-ETCHING AND
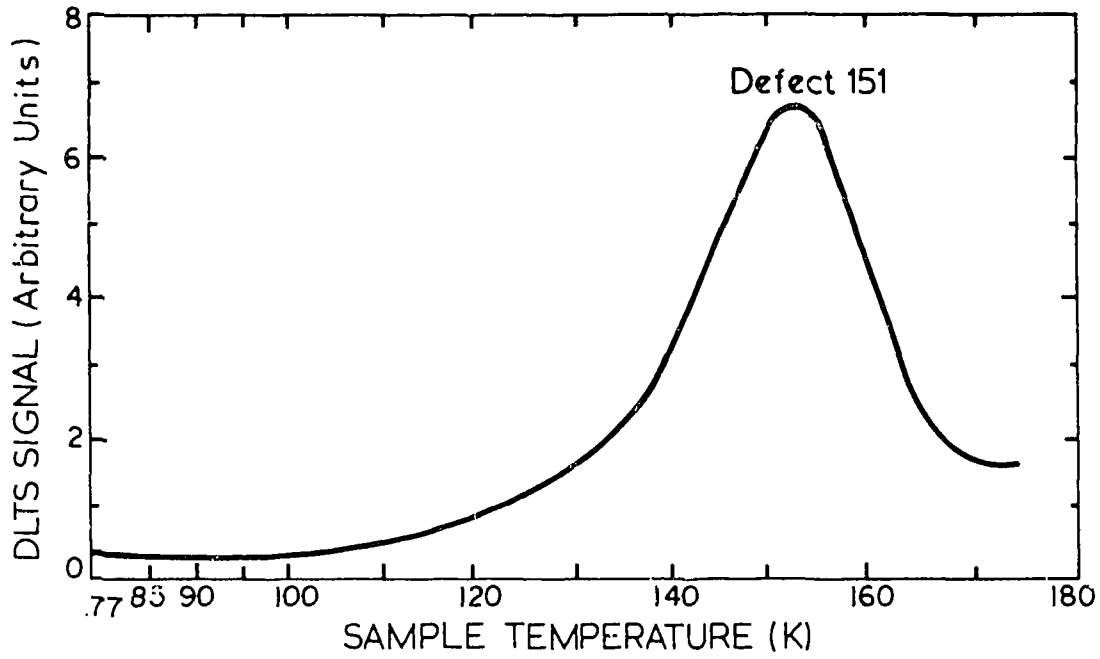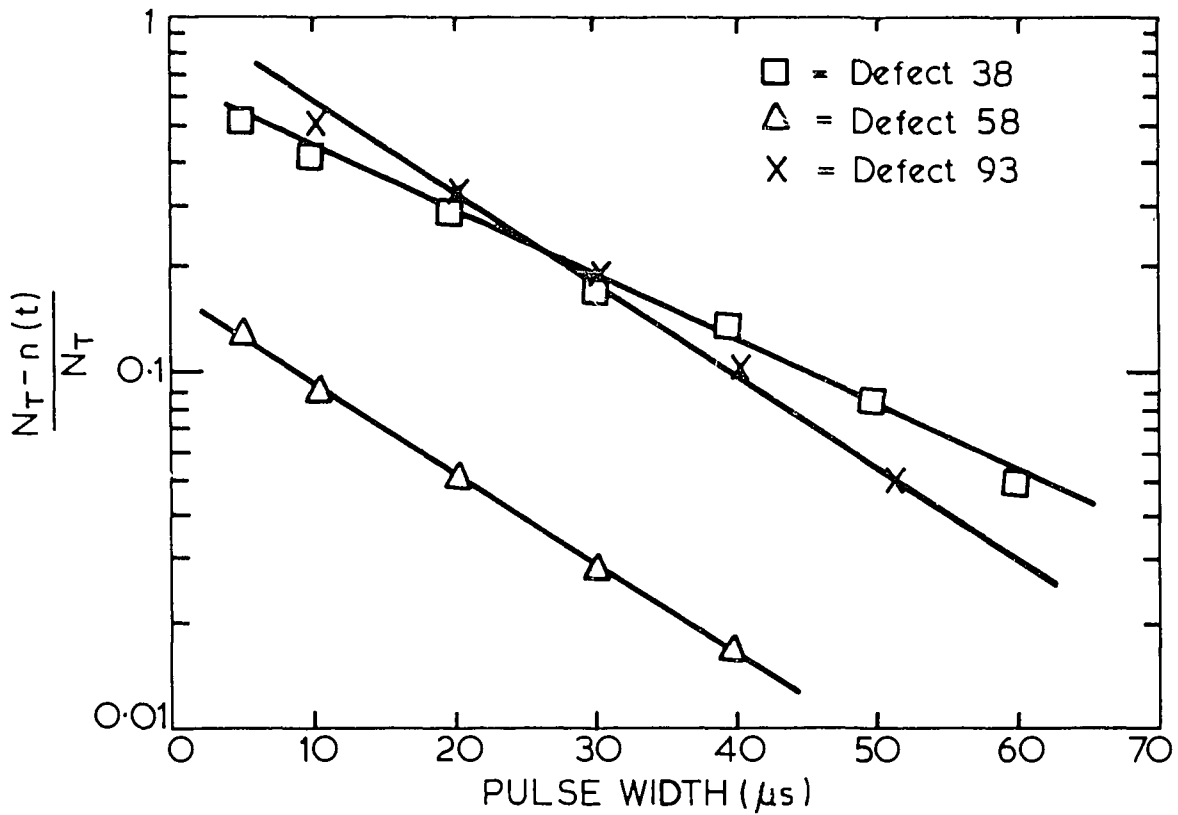EVAPORATION OF NEW Au BARRIER. (τ_c = 10 ms)

FIGURE 6. DLT SPECTRA OF SAMPLE Ge 2E AFTER IRRADIATION AND
THEN 10 YEARS AT ROOM TEMPERATURE ($\tau_c = 10$ ms)

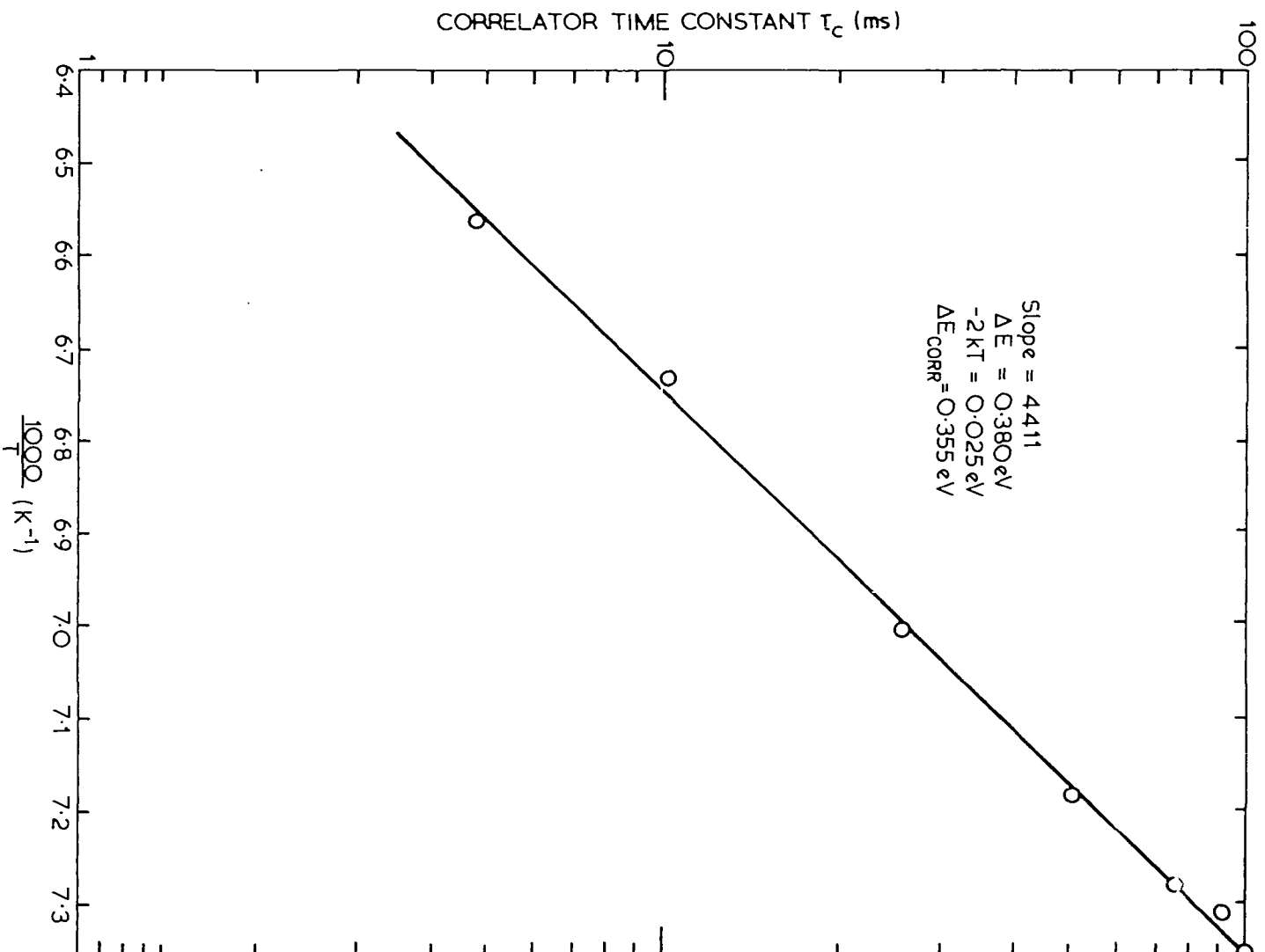FIGURE 7. RELATIVE SIGNAL OUTPUT v. PULSE WIDTH FOR
SAMPLE Ge 4D2

CORRELATOR TIME CONSTANT τ_c (ms)

Slope = 4411
ΔE = 0·380 eV
−2 kT = 0·025 eV
ΔE_{CORR}= 0·355 eV

$\frac{1000}{T}$ (K⁻¹)

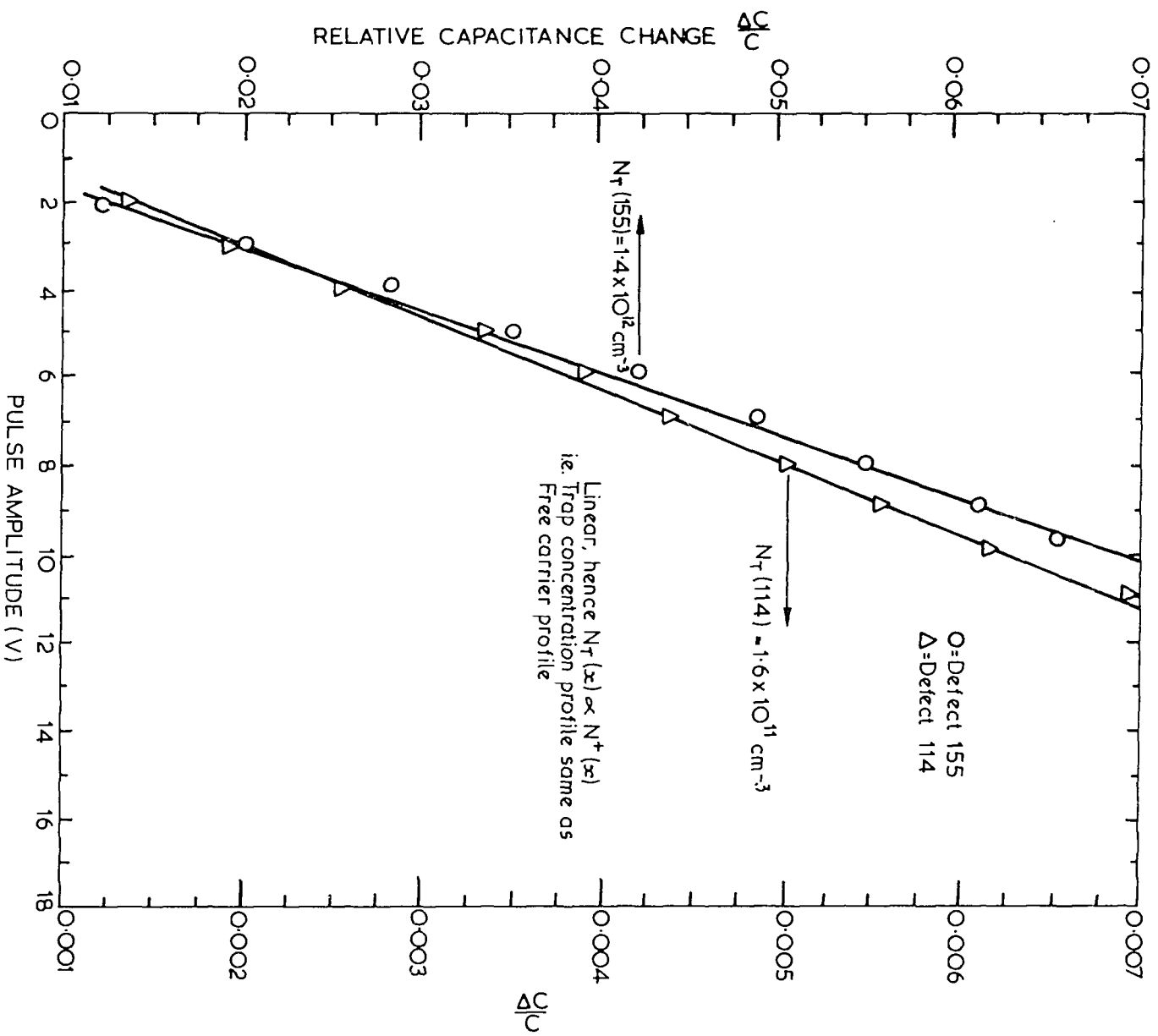FIGURE 8. ARRHENIUS PLOT FOR SAMPLE Ge 4D2 (defect 148)

23

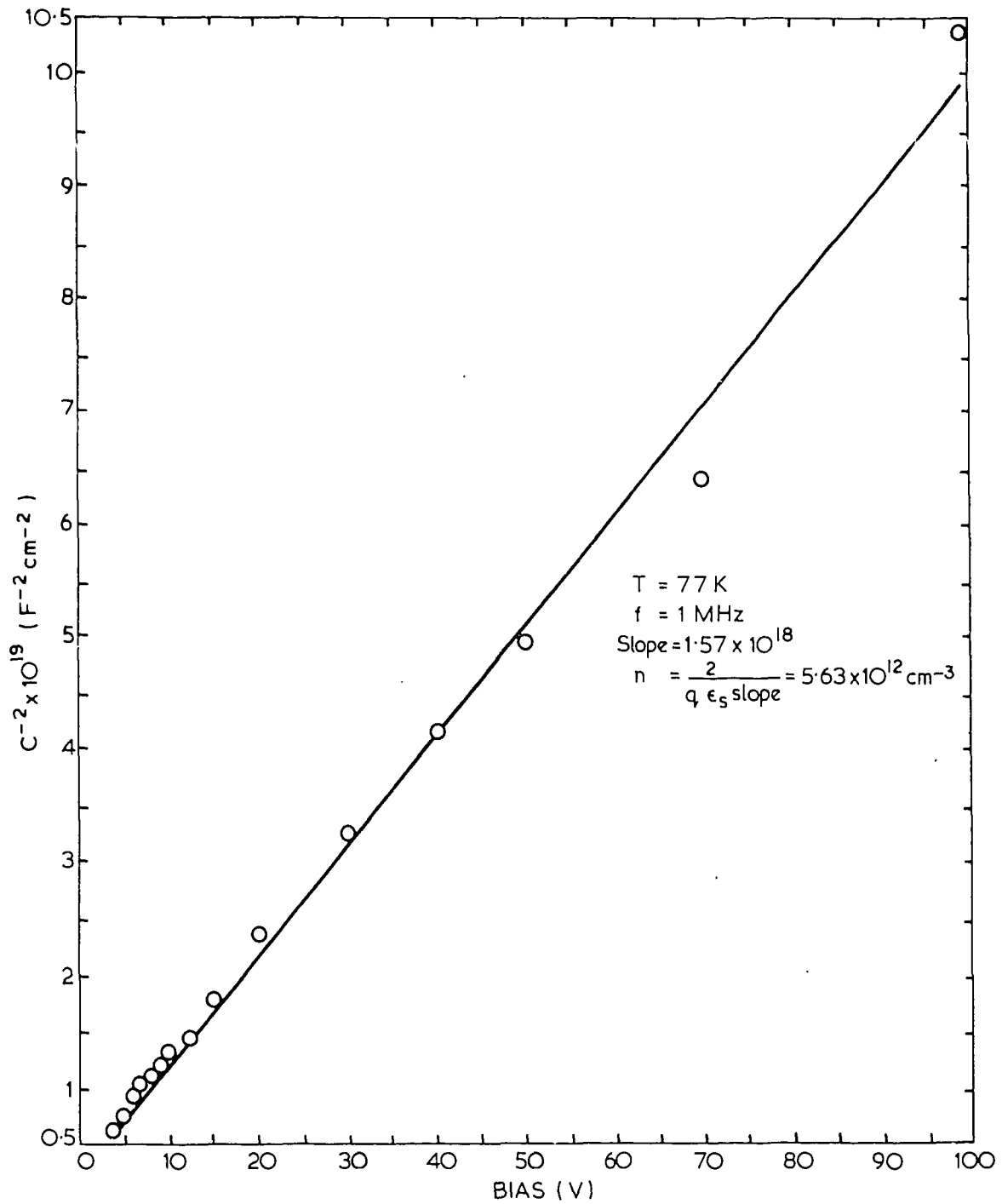FIGURE 9. RELATIVE CAPACITANCE CHANGE v. PULSE AMPLITUDE FOR SAMPLE Ge 5D

FIGURE 10. PLOT OF C^{-2} v. V FOR SAMPLE Ge 5D

The figure shows a plot with:
- Y-axis: $C^{-2} \times 10^{19}$ ($F^{-2}cm^{-2}$)
- X-axis: BIAS (V)
- Annotations: $T = 77\,K$, $f = 1\,MHz$, $Slope = 1 \cdot 57 \times 10^{18}$, $n = \dfrac{2}{q\,\epsilon_s\,slope} = 5 \cdot 63 \times 10^{12}\,cm^{-3}$